

## Chemical oxygen demand removal from electroplating wastewater by purified and polymer functionalized carbon nanotubes adsorbents



M.T. Bankole<sup>a,e</sup>, A.S. Abdulkareem<sup>b,e</sup>, J.O. Tijani<sup>a,e,\*</sup>, S.S. Ochigbo<sup>a</sup>, A.S. Afolabi<sup>c</sup>, W.D. Roos<sup>d</sup>

<sup>a</sup> Department of Chemistry, Federal University of Technology, PMB.65, Minna, Niger State, Nigeria

<sup>b</sup> Department of Chemical Engineering, Federal University of Technology, PMB.65, Minna, Niger State, Nigeria

<sup>c</sup> Department of Chemical, Materials and Metallurgical Engineering, Botswana International University of Science and Technology (BIUST), Plot 10071, Boseja ward, Palapye, Botswana

<sup>d</sup> Department of Physics, University of the Free State, P.O. Box 339, ZA-9300 Bloemfontein, South Africa

<sup>e</sup> Nanotechnology Research Group, Centre for Genetic Engineering and Biotechnology (CGEB), Federal University of Technology, P.M.B 65, Bosso, Minna, Niger State, Nigeria

### ARTICLE INFO

#### Keywords:

Electroplating wastewater  
Carbon nanotubes  
Functionalization  
Characterization  
Chemical oxygen demand

### ABSTRACT

This study investigated the removal of chemical oxygen demand (COD) from electroplating industry wastewater via batch adsorption by purified and polymers functionalized carbon nanotubes (CNTs) as nano-adsorbents. Bimetallic Fe-Co supported on CaCO<sub>3</sub> was utilized to produce multi-walled carbon nanotubes (MWCNT) via the catalytic chemical vapor deposition (CCVD) technique. This was subsequently followed by the purification of the as-prepared MWCNTs by a mixture of HNO<sub>3</sub> and H<sub>2</sub>SO<sub>4</sub> in order to remove the support and metal particles. The purified MWCNTs was further functionalized using known mass of the following polymers: Amino polyethylene glycol (PEG), polyhydroxylbutyrate (PHB) and amino polyethylene glycol with polyhydroxylbutyrate (PEG-PHB). The purified (P-CNTs) and functionalized CNTs coded PEG-CNTs; PHB-CNTs, and PEG-PHB-CNTs were characterized by HRSEM, HRTEM-EDS, BET, XRD and XPS. The electroplating wastewater was subjected to physicochemical characterization before and after treatment with various prepared nano-adsorbents using standard methods. The adsorption process under the influence of contact time, adsorbent dosage and temperature was measured using the chemical oxygen demand (COD) as indicator parameter. The HRSEM/XRD/BET confirmed that the purified and polymer functionalized CNTs were homogeneously dispersed; highly graphitic in nature with fewer impurities and of high surface area (> 145 m<sup>2</sup>/g). The order of maximum COD removal by the nano-adsorbents at equilibrium time of 70 min are as follows: PEG-CNTs (99.68%) > PHB-CNTs (97.89%) > P-CNTs (96.34%) > PEG-PHB-CNTs (95.42%). Equilibrium sorption data were better described by Freundlich isotherm with the correlation coefficient (R<sup>2</sup> > 0.92) than Langmuir isotherm. The adsorption kinetics for COD removal from electroplating wastewater fitted well to the pseudo-second-order model with rate constant in the range of 4 × 10<sup>-5</sup>–1 × 10<sup>-4</sup> (g mg<sup>-1</sup> min<sup>-1</sup>). Thermodynamics analysis of the adsorption process revealed that the enthalpy (ΔH°) of the reaction was positive and endothermic in nature. The Gibbs free energy (ΔG°) was negative which showed the feasibility and spontaneity

\* Corresponding author at: Department of Chemistry, Federal University of Technology, PMB.65, Minna, Niger State, Nigeria.

E-mail address: [jimohtijani@futminna.edu.ng](mailto:jimohtijani@futminna.edu.ng) (J.O. Tijani).

<http://dx.doi.org/10.1016/j.wri.2017.07.001>

Received 19 April 2017; Received in revised form 16 June 2017; Accepted 12 July 2017

2212-3717/© 2017 The Authors. Published by Elsevier B.V. This is an open access article under the CC BY-NC-ND license (<http://creativecommons.org/licenses/by-nc-nd/4.0/>).

of adsorption process. The findings from this study support the potential use of PEG-functionalised CNTs as a nanoadsorbent to purify electroplating wastewater than others prepared sorbents.

## 1. Introduction

Pollution of water sources via anthropogenic activities such as electroplating, smelting, manufacturing, petrochemicals and mining is considered as a global phenomenon threaten human survival and aquatic life and thus needs to be addressed using research and development [1,2]. The increased human population and consumer demands have been identified as possible factors responsible for the growing multiplications of industries and pollution status worldwide. One of such industries is the electroplating activity, which involves alkaline cleaning, acid pickling, plating, and rinsing and as such generate large volume of untreated wastewater especially at the rinse stage [2]. It is worthy to note that, the presence of spent acid and other coating constituents contributed significantly to the complexity of the treatment process [3]. Besides acidic components, electroplating wastewater contains different inorganic and organic species and direct discharge of such untreated liquid wastes into the hydrosphere posed serious danger to the ecosystem due to their toxic and recalcitrant nature [2]. Furthermore, Chowdhury et al. [4] submitted that value of water quality parameters such as chemical oxygen demand (COD), biochemical oxygen demand (BOD), high color contents, cyanide complexes and metal ions remain high in electroplating wastewater thus their reduction using conventional treatment techniques becomes difficult. It is important to mention that acidic or alkaline plating wastewater causes corrosion on the concrete structures while the suspended impurities clog the sewer system [5]. In the same vein, high concentrations of iron stain furniture, equipment and laundry. The health effect of exposure to electroplating wastewater include; necrosis and nephritis in the human body; irritation of the gastrointestinal mucosa and prolong exposure can cause lung cancer, digestive tract cancer, and maxillary sinus cancer [6,7]. Other problems associated with this kind of water pollution include destruction of water aesthetic value, reduction of photosynthetic activity and damage of food web remaining in water ecosystem [7]. In view of the negative environmental impacts of exposure to electroplating wastewater, there is a need to develop highly efficient and sustainable treatment techniques to remove hazardous constituent in the wastewater before discharge to aqueous bodies.

In the past, dilution technique is mostly practiced; however, the technique alone could not solve the problem. For instance, one hundred gallon of chromium plating solution diluted by 200,000,000 gallons of stream water still has high concentration of chromium ion that could destroy most aquatic life [7]. Besides the dilution technique, numerous other physicochemical methods such as electrochemical method [8], membrane process, chemical precipitation [9], reverse osmosis [10], ion exchange [10], coagulation, flocculation, ozonation [11], filtration amongst others have been applied globally in the treatment of electroplating wastewater. Till today, efforts are still ongoing to find an ideal, economic, effective and sustainable water treatment for commercial utilization because of the problems associated with the existing ones [12]. For instance, chemical precipitations generate large amounts of rich toxic sludge and even the removal of inorganic species is often low. Furthermore, the operation and maintenance cost due to sludge handling, generated during coagulation and flocculation processes is expensive [13]. The electrolytic deposition method also produces toxic residual cyanide compounds which may need further treatment. In contrast, adsorption technology is one of the most reliable, versatile and effective surface methods utilized by researchers to remove organic and inorganic constituents including microbes from wastewater [14]. The advantages of adsorption technology include simple design, easy of operation, none generation of toxic substances and easy recovery of the adsorbent after treatment to mention but a few [13,14]. Adsorbents such as activated carbon, zeolite, kaolin with different adsorption potentials have been known to remove organic and inorganic contaminants from wastewater released by industries [15]. These materials are considered because of their availability and abundance nature, higher adsorption capacity attributable to high porosity and large surface area [16]. However, high cost of commercial activated carbon (AC) and low regeneration efficiency limits its industrial applications for wastewater treatment. In view of the expensive nature of the commercial AC, there is need to develop alternative adsorbent with high surface area than AC [17]. Carbon nanotubes (CNTs) has emerged as a viable adsorbent for the removal both organic and inorganic matters from wastewater due to its unique small, hollow and tubular structure, high surface area and high aspect ratio [15,16]. Other properties of CNTs include high surface active site to volume ratio, controlled pore size distribution and outstanding sorption capacity compared to conventional granular and powder activated carbon [18]. Further studies show that the adsorption capacity of CNTs depends on both the surface functional groups and the nature of the sorbate [14–18]. Different researchers have explored CNTs as adsorbents to remove heavy metals, dyes, microbes and even emerging organic contaminants by both batch and column adsorption process [11–18]. For instance, Su and Lu [19] employed multi-walled carbon nanotubes (MWCNTs) and activated carbon to remove natural dissolved organic matter (NDOM) from aqueous solutions and established that MWCNTs prevented the microbial growths in drinking water than commercial activated carbon. Saleh and Gupta, [20] employed CNT/magnesium oxide composite to remove lead(II) from water via column adsorption process and found that under the optimum conditions of contact time and thickness of MnO<sub>2</sub>/CNT nanocomposite the flow rates of the feed solution was inversely proportional to the lead (II) removal rate. Su et al. [21] utilized oxidized multi-walled carbon nanotubes (MWCNTs) as adsorbent to remove benzene, toluene, ethylbenzene and p-xylene (BTEX) in aqueous solution. The authors revealed that sodium hypochlorite (NaOCl) modified MWCNTs exhibited greater adsorption capacity towards BTEX than commercial activated carbon under the same applied contact time and initial concentration. Veličković et al. [22] reported the removal of Cd(II), Pb(II) and As(V) ions from aqueous solution using unmodified and polyethylene glycol modified multi-walled CNTs (PEG-MWCNTs) and found that adsorption of the metal ions onto the adsorbents was pH dependent even though PEG-MWCNTs removed more metal

ions than unmodified MWCNTs. Gupta et al. [23] demonstrated the removal of lead ions from aqueous solutions in two modes via batch and fixed bed by Alumina-coated multi-wall carbon nanotubes (MWCNTs). The authors found that Aluminium coated MWCNTs exhibited excellent removal of lead ions compared to uncoated and that increasing the thickness and decreasing the flow rate improved lead removal rate. Saleh et al. [24] compared the adsorptive capacity of silica/carbon nanotubes (CNTs) and silica/activated carbon (AC) for removal of mercury ions from aqueous solutions. They found that silica/CNT removed mercury more than silica/AC and the equilibrium adsorption data fitted Freundlich isotherm more than Langmuir and Temkin isotherms. Saleh et al. [25] used MWCNT and SiO<sub>2</sub> individually and their combination as adsorbent to sequester Pb(II) from aqueous solutions and revealed that combined MWCNT/SiO<sub>2</sub> composite adsorbed (~95%) of Pb(II) compared to silica nanoparticles and CNTs that ordinarily eliminated (~50%) and (~45%) respectively under the same conditions.

Despite the uniqueness of MWCNTs as an adsorbent, aggregation/agglomeration of carbon nanomaterials in the aqueous matrix still remains a challenge [25]. To solve this problem, adequate dispersion to ensure proper interaction of CNTs with the contaminants in wastewater is necessary in order to enhance its adsorption potentials and also improve the intrinsic properties of nanotubes material. Various dispersion methods have been reported namely surfactant-treated dispersion, surface-modified dispersion and polymer wrapping amongst others [26]. The first two methods have associated shortcomings such as post-surfactant removal for subsequent uses and even damage of the CNTs surface. On the other hand, polymer functionalisation technique based on ultrasonication effect have been found to reduce these surface defects due to introduction of more functional groups that enhance the adsorptive potentials of the tubular materials. Not only that, the functionalization improves the solubility, stability, dispersion rate and electrical conducting ability of the CNTs. Various polymers have been used to improve the rate of dispersion of CNTs in water however in this study Amino polyethylene glycol (PEG) polyhydroxybutyrate (PHB) and amino polyethylene glycol with polyhydroxybutyrate (PEG-PHB) were selected [26]. The choice of amino PEG was based on its nucleophilicity and ability to easily form amide bond with organic and inorganic substrates. In the same vein, PHB was preferred over other polymers due to its good oxygen permeability, less stickiness in aqueous solution and resistant to hydrolytic degradation. It is envisaged that the blending or incorporation of the two polymers onto the cylindrical hollow structure would create synergy and overcome the surface defects in CNTs.

To the best of our knowledge, COD removal by purified and polymer functionalised CNTs from electroplating wastewater has not been reported by any author. This research provides a new insight on the adsorption mechanism of COD from electroplating wastewater using purified and polymer functionalized CNTs. Thus, the originality lies in the functionalization of the acid purified CNTs with three different polymeric materials namely: Amino polyethylene glycol (PEG), polyhydroxybutyrate (PHB) and amino polyethylene glycol with polyhydroxybutyrate (PEG-PHB) and subsequent utilization for COD removal from electroplating wastewater using batch adsorption process. The as-prepared and polymer functionalized carbon nanostructure materials were characterized for their morphologies, microstructures, specific surface areas, elemental composition, crystallinity and surface elemental oxidation states using High Resolution Scanning Electron Microscope (HRSEM), High Resolution Transmission Electron Microscope (HRTEM) along with an Energy Dispersive X-ray Spectrometer (EDS), Multi-point Brunauer–Emmett–Teller (BET) analyses and N<sub>2</sub> adsorbate measurements, X-ray diffraction (XRD) and X-ray Photoelectron Spectroscopy (XPS) analysis.

## 2. Materials and methods

### 2.1. Chemicals and materials

Chemicals used in this study include calcium trioxocarbonate (IV), cobalt (II) trioxonitrate (V) hexahydrate, iron (III) trioxonitrate (V) nonahydrate, hydrogen tetraoxosulfate (VI) acid, hydrogen trioxonitrate (V) acid, dimethylformamide (DMF), thionyl chloride, polyhydroxybutyrate, methanol, and sodium hydrogen trioxocarbonate (V) which were obtained from Sigma Aldrich. Liquid nitrogen, acetylene, argon and nitrogen gases were purchased from British Oxygen Company/Brin's Oxygen Company (BOC Gases Nigeria Plc, Lagos). All the chemicals were analytical grade with percentage purity in the range of 98 – 99.99% and used without further purification. Distilled and de-ionized water was obtained from the Centre for genetic engineering and biotechnology, Federal University of Technology, Minna, Nigeria.

### 2.2. Preparation of catalyst

The bimetallic catalyst, Fe-Co on CaCO<sub>3</sub> support was prepared by wet impregnation method [14]. In this study, 3.62 g and 2.47 g of nitrate salts of Iron and Cobalt compounds, Fe(NO<sub>3</sub>)<sub>3</sub>·9H<sub>2</sub>O and Co(NO<sub>3</sub>)<sub>2</sub>·6H<sub>2</sub>O were weighed and dissolved in 50 cm<sup>3</sup> of distilled water in 250 cm<sup>3</sup> volumetric flask corresponding to 0.18 and 0.17 M respectively. This was followed by the addition of 10 g of CaCO<sub>3</sub> to the same volume of distilled water (2 M solution) under continuous stirring at 2000 rpm for 60 min. The resulting slurry was then allowed to dry at room temperature after which it was dried in an oven at 120 °C for 12 h., cooled to room temperature, ground and finally screened through a 150 μm sieve. The final powder was then calcined at 400 °C for 16 h. The dried catalyst was ground to avoid agglomeration.

### 2.3. Production of carbon nanotubes (CNTs)

Carbon nanotubes were synthesised by the decomposition of acetylene gas in a CVD reactor on Fe-Co/CaCO<sub>3</sub>. A known weight (0.5 g) of the Fe-Co catalyst on CaCO<sub>3</sub> support was placed in the ceramic boat, which was inserted in the horizontal quartz tube of the

CVD furnace and heating was done at 10 °C/min. The heating commenced and argon was allowed to flow over the catalyst at a flow rate of 30 ml/min to purge the system of air. Once the temperature of 700 °C was reached, the argon gas was flown at rate of 230 ml/min followed by the introduction of acetylene gas at a flow rate of 190 ml/min for reaction time 60 min. After which the flow of acetylene was stopped and the furnace was allowed to cool to room temperature under continuous flow of argon. The ceramic boat was then removed and weighed to determine the quantity of CNTs produced. Percentage of CNTs yield was determined using the relationship provided independently by Yeoh et al. [15], and Taleshi [16] as presented in Eq. (1).

$$CNTs_{yield}(\%) = \frac{M_{Total} - M_{Catalyst}}{M_{Catalyst}} \times 100\% \quad (1)$$

where  $M_{Total}$  is the total mass of the catalyst and final carbon products after CVD reaction process and  $M_{Catalyst}$  is the initial mass of Fe-Co/CaCO<sub>3</sub> catalyst.

#### 2.4. Purification and functionalization of carbon nanotubes

The as-synthesised CNTs were treated with a concentrated HNO<sub>3</sub> and H<sub>2</sub>SO<sub>4</sub> mixture (v/v 1:3), by sonication for 3 h at 40 °C in an ultrasonic bath to introduce oxygen groups to the surface of the CNTs. The oxidized CNTs were cooled to room temperature and added slowly to 300 cm<sup>3</sup> cold deionized water, and filtered through a PTFE 0.22 μm pore size membrane filter. The filtrate was washed with deionized water until the pH became neutral and was oven dried at 80 °C for 8 h to give purified carbon nanotubes (P-CNTs). A known mass of the oxidized CNTs was dispersed in a known volume of anhydrous DMF (Dimethylformamide) under fume cupboard. Thionyl Chloride (SOCl<sub>2</sub>) was added and dispersed in an ultrasonicator for 15 min and transferred to a magnetic stirrer for 3 h at 50 °C, the dispersion was further heated at same temperature for 24 h. The obtained product was filtered with excess anhydrous tetrahydrofuran (THF) using a PTFE 0.22 μm pore size membrane filter. The CNT-COCl formed was dried in an oven at 60 °C for 3 h. A known mass of PEG-NH<sub>2</sub> (PEG-6-arm amino polyethylene glycol) and PHB (Polyhydroxybutyrate) were dispersed differently, and both combined in an anhydrous DMF (known mass) in a vial flushed with Nitrogen and protected against moisture. The CNT-COCl was added into the reaction mixture heated at 35 °C for 72 h using a magnetic stirrer. The obtained product was vacuum filtered and later dispersed by sonication in 5% NaHCO<sub>3</sub> and centrifuged twice continually. After the centrifuging, the supernatant was removed, and the precipitate dispersed in deionized water by sonication, and filtered using a PTFE 0.22 μm pore size membrane filter. There was extensive washing of the filtrate with deionized water and methanol, followed by drying in a vacuum oven at 60 °C for 3 h to give functionalized (nano-adsorbent); Amino polyethylene glycol functionalized carbon nanotubes (PEG-CNTs), polyhydroxybutyrate functionalized carbon nanotubes (PHB-CNTs) and amino polyethylene glycol with polyhydroxybutyrate functionalized carbon nanotubes (PEG-PHB-CNTs). Due to the polymerization degree; the dried products were ground for further use in adsorption experiments.

#### 2.5. Characterization of the wastewater

Industrial wastewater was collected from Electroplating section, SEDI, Minna, Niger State, Nigeria. Immediately after collection, the wastewater was subjected to characterization. All the analyses were carried out on the recommendation of standard methods of water and wastewater analysis. The inorganic composition method was determined using American Public Health Association (APHA) method [17]; Turbidity (Turbidity Meter), pH (a multi-parameter analyser C3010), electrical conductivity (a multi-parameter analyser C3010), dissolved oxygen (DO) (DO<sub>2</sub> Meter), chemical oxygen demand (COD), biochemical oxygen demand (BOD), total dissolved solid (TDS), alkalinity, the total amount of nitrate, nitrite, sulfate, phosphate, ammonium, chloride, cyanide and fluoride were determined using instruments by HACH, USA. All these analyses were carried out at Regional Water Quality laboratory, Federal Ministry of Water Resources, Minna. Adsorption capacities of purified CNTs (P-CNTs), and functionalized CNTs; PHB-CNTs, PEG-CNTs and PEG-PHB-CNTs were investigated using a batch adsorption process in the wastewater treatment.

#### 2.6. Batch adsorption experiment

Batch adsorption experiments of chemical oxygen demand (COD), which include the effect of contact time, adsorbent dosage, and temperature on the electroplating wastewater were carried out in this work. Batch experiments were carried out at 25 °C by adding known weight of nano-adsorbents into a number of 100 cm<sup>3</sup> glass stoppered conical flasks on a rotary shaker at 190 rpm containing 50 cm<sup>3</sup> of the electroplating wastewater. The effect of contact time was conducted by shaking 0.01 g of nano-adsorbents and 50 cm<sup>3</sup> of the electroplating wastewater at different time (10, 20, 30, 40, 50, 60, 70, and 80 min). The effect of adsorbent dosage was investigated by adding varying amounts of nano-adsorbents (0.01, 0.02, 0.03, 0.04, and 0.05 g) to 50 cm<sup>3</sup> of the electroplating wastewater at 70 min shaking time. To determine the effect of temperature, 0.01 g of nano-adsorbent was agitated in a flask containing 50 cm<sup>3</sup> for 70 min in a thermostat controlled water bath shaker operated at varying temperature (303, 313, 323, 333, and 343 K) and shaking at 190 rpm to reach equilibrium. All experiments were done in duplicate and the mean values are presented. The data analysis was on one-way analysis of variance (ANOVA) using SPSS 11.5 for Windows. The percentage of adsorption of COD was calculated using Eq. (2).

$$COD \text{ removal}(\%) = \frac{C_0 - C_e}{C_0} \times 100 \quad (2)$$

Where  $C_0$  is the initial COD concentration (mg/L) and  $C_e$  is the COD equilibrium concentration (mg/L).

## 2.7. Characterization of the nano-adsorbents

The mineralogical composition of as-synthesised catalyst and MWCNTs were identified using powder X-ray diffraction analysis, performed on a Bruker AXS D8 Advance with Cu-K $\alpha$  radiation with the acceleration voltage 40 kV, and scan velocity current 40 mA. A portion of the crystals were sprinkled on a de-greased glass slide, and diffractograms were recorded between diffraction angles (2 theta values) of 20° and 80°. The morphologies of the as-prepared materials were examined using Zeiss Auriga HRSEM under the following operation conditions: current 10 mA, voltage 5 kV, aperture 0.4 mm and working distance 4 – 10.4 mm. A mass of 0.05 mg prepared samples were sprinkled on carbon adhesive tape and sputter coated with Au-Pd using Quorum T150T for 5 min prior to analysis. The microscope was operated with electron high tension (EHT) of 5 kV for imaging. HRSEM equipped with EDS was further used to determine the elemental composition of the synthesised catalysts. The microstructure determination of the prepared catalysts and MWCNTs were done using a Zeiss Auriga High resolution transmission electron microscope (HRTEM) under the following measurement conditions: emission current (54  $\mu$ A), extraction voltage (3950 V), resolution (0.24 nm), magnification (varied), spot size (3 mm). Approximately 0.02 g of the synthesised products was suspended in 10 ml methanol and thereafter subjected to ultrasonication until complete dispersion was achieved. One or two drops of the slurry was dropped onto a holey carbon grid with the aid of a micropipette and subsequently dried via exposure to photo light prior to imaging. For BET N<sub>2</sub> adsorption, about 100 mg of the dry CNTs in a sample tube was first degassed at 90 °C for 4 h to remove residual water and other volatile components that were likely to block the pores. The N<sub>2</sub> adsorption-desorption isotherms were collected at –196 °C using Micromeritics ASAP 2020 Accelerated Surface Area and Porosimetry analyser. A XPS PHI 5400 equipped with hemispherical sector analyser operated using non-monochromated Al K $\alpha$  X-rays with an energy of 1486.6 eV at 300 W and 15 kV was used to examine the surface composition of the material. The energy scale was calibrated using Au 4f<sub>7/2</sub> at 83.95 eV, and the linearity of the scan was adjusted to measure Cu 2p<sub>3/2</sub> at a position of 932.63 eV. Surveys were scanned (2.5 eV/s) with a pass energy of 178 eV, and detail spectra were collected with a pass energy of 44 eV and a scan rate of 0.625 eV/s. The photoelectron take-off angle for all measurements was 45°. All spectra obtained were energy corrected using the aliphatic adventitious hydrocarbon C (1s) peak at 284.8 eV. The XPS Peak 4.1 software (<http://xpspeak.software.informer.com/4.1/>) was used for data analysis and fits.

## 3. Results and discussion

### 3.1. Physicochemical parameters of the electroplating wastewater

Prior to the batch adsorption study on the electroplating wastewater, the physicochemical parameters of the wastewater were analyzed and the results obtained are presented in Table 1.

The results presented in Table 1 indicate that the pH of the raw effluent was 0.83, which is highly acidic because of the acid

Table 1

The mean concentration of physicochemical characteristics of electroplating wastewater (before and after adsorption process) and compare with standard permissible limits.

Physicochemical parameters	Raw value before treatment	Values after treatment using P-CNTs	Values after treatment using PHB-CNTs	Values after treatment using PEG-CNTs	Values after treatment using PEG-PHB-CNTs	Standard limits (WHO/EPA)	Standard limits (NIS)
Ph	0.83	5.63	5.65	5.88	5.36.00	5.5–8.5	6.5–8.5
TDS (mg/L)	1915.00	462.30	422.10	408.70	475.70	600	500.00
Conductivity ( $\mu$ S/cm)	2860.00	690.00	630.00	610.00	710.00	1000	1000.00
Turbidity (NTU)	256.00	2.00	2.00	2.00	4.00	5	5.00
Dissolved Oxygen (mg/L)	4.00	5.71	5.70	5.80	5.68	5–6	–
Total Alkalinity (mg/L)	100.00	10.00	9.00	9.00	12.00	–	–
Nitrate (mg/L)	891.00	123.00	107.00	98.00	135.00	50	50.00
Ammonia (mg/L)	150.00	8.11	7.59	5.99	9.00	1.5/0.5	–
Chloride (mg/L)	550.00	40.00	38.50	38.00	49.00	250.00	–
Phosphate (mg/L)	278.00	6.03	5.32	4.95	6.65	0.50	–
Cyanide (mg/L)	180.00	1.53	1.11	1.03	1.80	0.05	0.01
Fluoride (mg/L)	305.00	1.21	1.09	1.05	1.33	1.5/1	1.50
Sulfate (mg/L)	1800.00	79.00	78.00	74.00	85.00	250/200	100.00
COD (mg/L)	1094.00	23.00	10.00	3.50	48.00	40.00	–
BOD <sub>5</sub> (mg/L)	1.56	1.00	1.00	0.50	1.50	10/5–7	–
Carbonate (mg/L)	0.00	0.00	0.00	0.00	0.00	–	–
Nitrite (mg/L)	5.70	0.20	0.09	0.09	0.20	3/0.05	2.00
Total Bacteria Count (cfu/ml)	0.00	0.00	0.00	0.00	0.00	–	–

Key: World Health Organization (WHO) [18], Environmental Protection Agency (EPA) [19] and Nigerian Industrial Standard (NIS) [20].

prickling method adopted for electroplating activity. However, after treatment with the nano-adsorbents, the pH increased and was in the range of 5.36–5.88, with PEG-CNTs treatment having the highest pH value. pH affects the solubility, mobility and toxicity of chemicals and heavy metals in the water, and often increase the risk of absorption by aquatic life. When the pH of water is too high or too low, the aquatic organisms living within it will die. The majority of aquatic creatures prefer a pH range of 6.5–9.0, while humans have a higher tolerance for pH levels (drinkable levels range from 4 to 11 with minimal gastrointestinal irritation) [27]. The recommended pH range for most fish is between 6.0 and 9.0 with a minimum alkalinity of 20 mg/L. However, most grasses and legumes prefer soils with a pH of 4.5–7.0. Some amphibians can often tolerate pH levels as low as 4.0. According to Fondriest environmental [27], the treated water in this study can be used for irrigation activities. From Table 1, the total alkalinity of the raw wastewater was 100 mg/L and after treatment reduced to the range of 9–12 mg/L. Furthermore, the ammonia (NH<sub>3</sub>) content of the untreated wastewater is 150 mg/L. After treatment the NH<sub>3</sub> levels reduced to the range of 5.99–9 mg/L. High levels of ammonia in water can lead to death of aquatic species especially when the pH is 9.0. At a pH > 9, ammonia is released into the water which is extremely toxic to aquatic organisms. Although the pH, alkalinity and ammonia ranges obtained after treatment did not meet the standard requirements for drinking water, it is fit for agricultural purposes. Turbidity in water is caused by suspended and colloidal matter such as silt, clay, finely divided organic and inorganic matter, and other microscopic organisms, which affects the conductivity of water system. Prior to the treatment of the electroplating wastewater, the turbidity value was 256 NTU. After treatment a drastic reduction in the turbidity values in the range of 2–4 NTU was achieved. This result falls within the maximum permissible limit for safe water [28] and WHO and EPA reported a safety limit of 5 NTU [28,29]. The conductivity of water is a linear function of the concentration of dissolved ions, which serve as an indicator of water quality and an increase in the conductivity of water is an indication of presence of dissolved ions [30]. The conductivity value of the raw effluent was 2860  $\mu$ S/cm, which was reduced to 690  $\mu$ S/cm, 630  $\mu$ S/cm, 610 and 710  $\mu$ S/cm after the treatment with P-CNTs, PHB-CNTs, PEG-CNTs and PEG-PHB-CNTs respectively. In this study, TDS of the raw effluent is 1915 mg/L, and after the treatment the TDS value range from 408.7 to 475.7 mg/L (Table 1) and of all the nano-adsorbents, PEG-CNTs exhibited the least removal efficiency. The values obtained after the treatment, falls below WHO/EPA and NIS maximum limits. According to NIS [30], the maximum permissible limit of TDS is 500 mg/L for drinking water, while aquatic animals in freshwater and salmons can still withstand 2000 mg/L and 3600 mg/L. In summary, the four nano-adsorbents were able to remove approximately 97% of TDS from the electroplating effluent. In Table 1, it was noticed that the DO value of the electroplating wastewater before treatment was 4 mg/L and in the range of 5.68–5.8 mg/L after treatment, with PEG-CNTs exhibited the highest value. The results obtained meet the recommended limit of 5–6 mg/L [27]. Furthermore, the amount of DO is inversely proportional to the BOD. According to European Union directive, 5–7 mg/L of BOD is the maximum permissible limit for safe water [27] and WHO reported safe limit of 10 mg/L [26]. The BOD levels reported in Table 1, both before and after treatment, fall within the maximum permissible limits. The COD gives an estimate of the organic matter present in a water body [24]. According to the results in Table 1, the COD value of electroplating wastewater is 1094 mg/L, which is above the safe discharge limit set by the

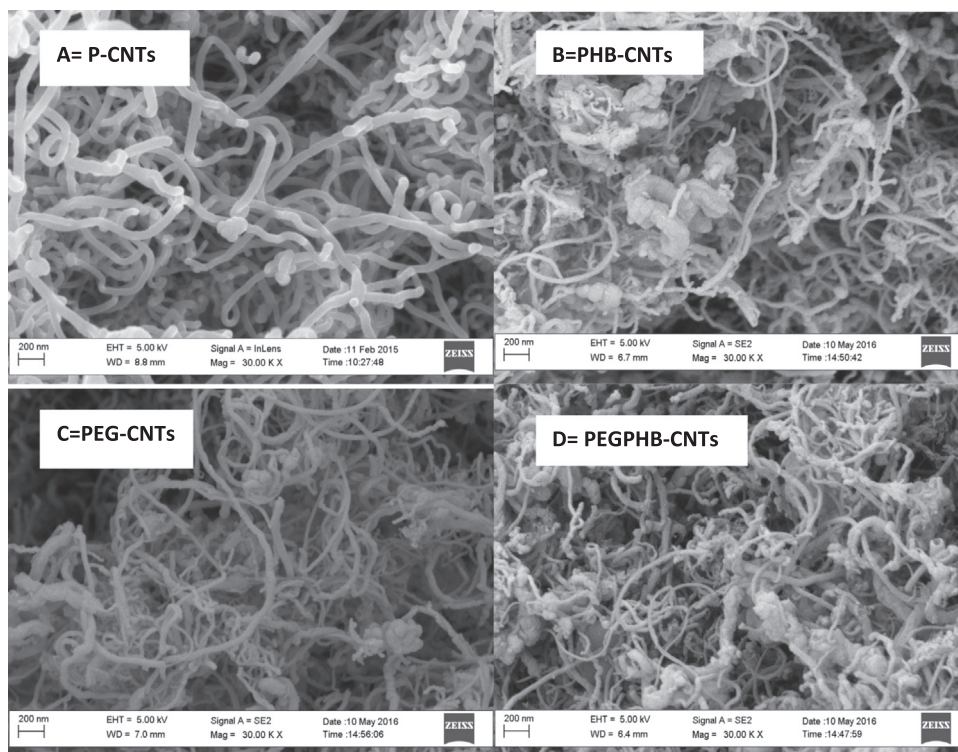


Fig. 1. High resolution scanning electron microscope images of the purified and functionalized carbon nanotubes before treatment.

European Union and even NIS. However, after the adsorption process by the prepared nano-adsorbents, the COD values ranged from 3.5 to 48 mg/L, with PEG-CNTs that showed the highest COD removal potential. As shown in Table 1, the nitrate level of electroplating wastewater was 891 mg/L. After the adsorption process, the nitrate value ranged from 98 to 135 mg/L, with PEG-CNTs treatment having the lowest nitrate value. This result did not fall within the standard permissible limit, but there was approximately 89% removal of nitrate by the nano-adsorbents. The presence of nitrate in the water samples is due to its usage as a corrosion inhibitor in industrial process water. The nitrite level in the electroplating wastewater was 5.7 mg/L and after the treatment the values were in the range of 0.09–0.2 mg/L, which is below the permissible limit. Furthermore, the phosphate level in the electroplating wastewater was 278 mg/L prior to the treatment and subsequently decreased to between 4.95 and 6.65 mg/L after treatment depending on the nano-adsorbents. The value obtained did not fall within the maximum permissible limit of 0.5 mg/L [29]. It must be mentioned that the presence of nitrates and phosphate beyond a recommended limit in effluent water may be linked to the algae growth. According to Table 1, the concentration of cyanide is 180 mg/L, however after treatment; the concentration was reduced to a range of 1.03–1.8 mg/L. This implies that cyanide content fails to meet the standard limit in spite of 99–99.42% decrease achieved using the nano-adsorbents. More so, the sulfate concentration in the water sample is 1800 mg/L and after treatment, the value reduced to between 74 and 85 mg/L, which according to WHO [27] and EPA [29] satisfies the maximum permissible limit of 250 mg/L and 200 mg/L respectively. In the same vein, Table 1 reveals that the concentration of chloride in the untreated sample is 550 mg/L. After the adsorption processes, it is within the standard permissible limits of 38–49 mg/L.

### 3.2. Characterization of the Purified and Functionalized CNTs (Nano-adsorbents)

Shape, size and purity are vital in the identification characteristics of any type of adsorbents; these parameters directly affect the specific surface area and also influence the adsorption capacity of the adsorbents presented in Fig. 1. Fig. 1 represents the HRSEM micrographs of the purified and functionalized carbon nanotubes prior to the application for adsorption process.

It is observed from the HRSEM images shown in Fig. 1 that the isolated P-CNTs (pristine) have homogeneously distributed and dense smooth cylindrical shapes. The observed morphologies may be linked to the purification procedure adopted which ensured the removal of impurities such as the support material ( $\text{CaCO}_3$ ) and metallic residues (Fe, Co). Other authors attributed the formation of clean and smooth CNTs to the existence of inter-molecular forces within the isolated CNTs which possess different sizes, tubular-like and an aggregated formed structure. On the contrary, the polymer functionalized CNTs namely; (PHB-CNTs, PEG-CNTs and PEGPHB-CNTs) have rough thick clusters and aggregated morphologies as evidence on the outer surface wall of the CNTs [20]. The observed thick cluster was also observed in the HRTEM images show in Fig. 3. For instance, the rough cluster was more pronounced in the PHB-CNTs and PEGPHB-CNTs than PEG-CNTs. The possible reason may be due to the higher molecular weight and non-solubility of PHB in water than PEG, which resulted to the suppression and partial destruction of the CNTs morphologies. It should be mentioned that

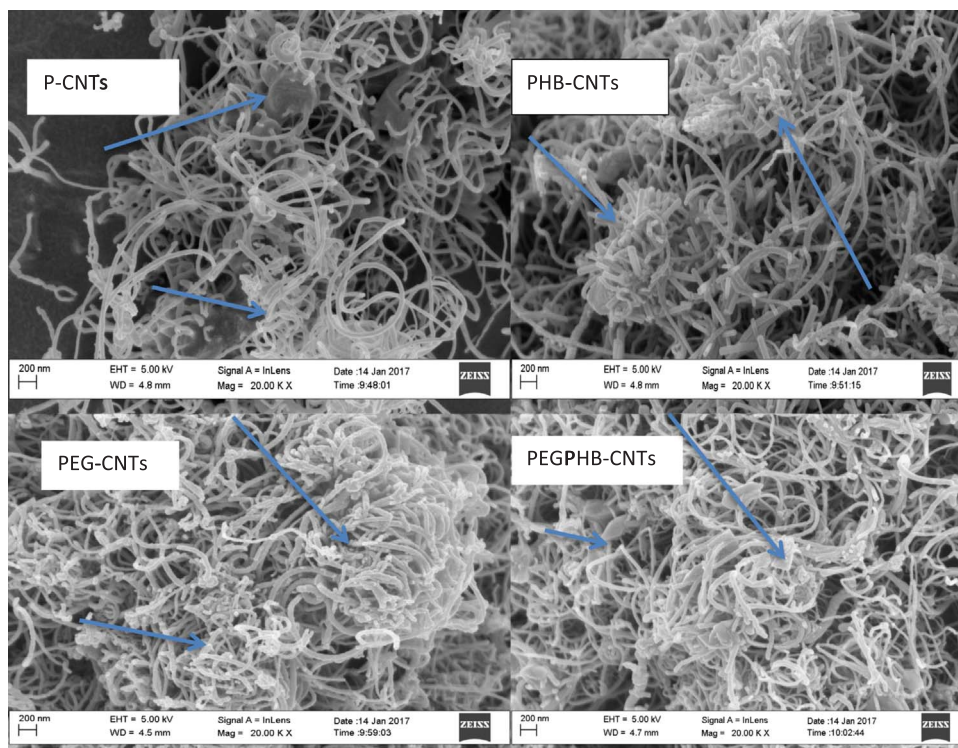


Fig. 2. High resolution scanning electron microscope images of the purified and functionalised carbon nanotubes used after the treatment of electroplating wastewater.

the HRSEM morphologies of PHB-CNTs and PEGPHB-CNTs are somehow similar and it was difficult to notice and even distinguish PHB-CNTs and PEGPHB-CNTs. This is because the PHB which is denser; exhibited matrix and adsorption effects other than PEG on the CNTs. The morphologies of the developed adsorbent was examined after the utilization for wastewater treatment and the results of the HRSEM analysis is presented in Fig. 2.

It could be seen from Fig. 2 that the curve and cylindrical shapes of the CNTs observed in Fig. 1 is still retained after the treatment under the applied conditions. The rough thick clusters and agglomerated morphologies observed especially for PHB, PEG and PEGPHB-CNTs prior to adsorption, disappeared without destroying the shapes of CNTs. This shows that functionalization using polymers did not destroy the CNTs morphologies. However, slight effects of CNTs cuts, breakages and shortening were observed while the inter-molecular forces within the isolated CNTs were reduced possibly due to adsorption of pollutants onto the surface of the outer-wall of the aggregated CNTs structure [23]. The clustering on the surface of the outer-wall of the CNTs increases forming a shining flake-like structure at its tip as indicated by arrows. Presented in Fig. 3 is the HRTEM image of the purified and functionalized CNTs. According to Fig. 3, multiple graphitic layers (multi-wall) structures (MWCNTs) with hollow inner diameters of 5.5 nm and defective etching at the outer edges of the walls were observed in all the samples.

It was found that the polymers are encapsulated within the lattice fringes of the polymer functionalized CNTs shown in Fig. 3 except for the P-CNTs. The presence of thick black clusters further supports non-solubility or miscibility of the polymer matrix with the CNTs [31]. Conversely, the black spot observed in the P-CNTs may be ascribed to the impurities which emanated either from catalyst or the support. These impurities were encapsulated within the wall of the CNTs as established by XPS results shown in Fig. 6. The EDS analysis was done to further confirm the elemental composition of the four nano-adsorbents and the results obtained are shown in Table 2. It can be noticed that the major and dominant elements in the four nano-adsorbent is carbon (C). The other residual elements; cobalt (Co) and iron (Fe) that locked up within the wall of the nanotube are the catalyst used to grow the CNTs in the CCVD while calcium (Ca) originated from the support ( $\text{CaCO}_3$ ). Sulfur emanated from the  $\text{H}_2\text{SO}_4$  used during purification.

BET surface area, pore size and pore volume of the purified and functionalized CNTs were determined using BET -  $\text{N}_2$  adsorption-desorption and the results are given in Table 3.

Nitrogen adsorption-desorption is frequently used to probe porosity and surface area of porous materials in BET analysis. The sorption isotherms of nitrogen on the four nano-adsorbents at 77 K and relative pressures ( $P/P_0 = 5.84 \times 10^{-2}$  to 0.307) are of type II (mesoporous). The specific surface area and porosity as shown in Table 3 are in the order of PHB-CNTs > P-CNTs > PEGPHB-CNTs > PEG-CNTs. After purification, an increase in the surface area and porosity was observed for the P-CNTs. However, on further functionalization with polymers, it was believed that the polymer would be aggregated on the external surface of the CNTs and blocks the pore, thereby caused reduction in surface area and porosity (see Fig. 1). This trend was observed for PEG-CNTs and PEGPHB-CNTs except PHB-CNTs. This is due to the excellent oxygen permeability and less stickiness of PHB on CNTs compared to others [31]. This might have contributed to the increment in surface area and porosity noticed in PHB-CNTs (see Table 3). The aforementioned

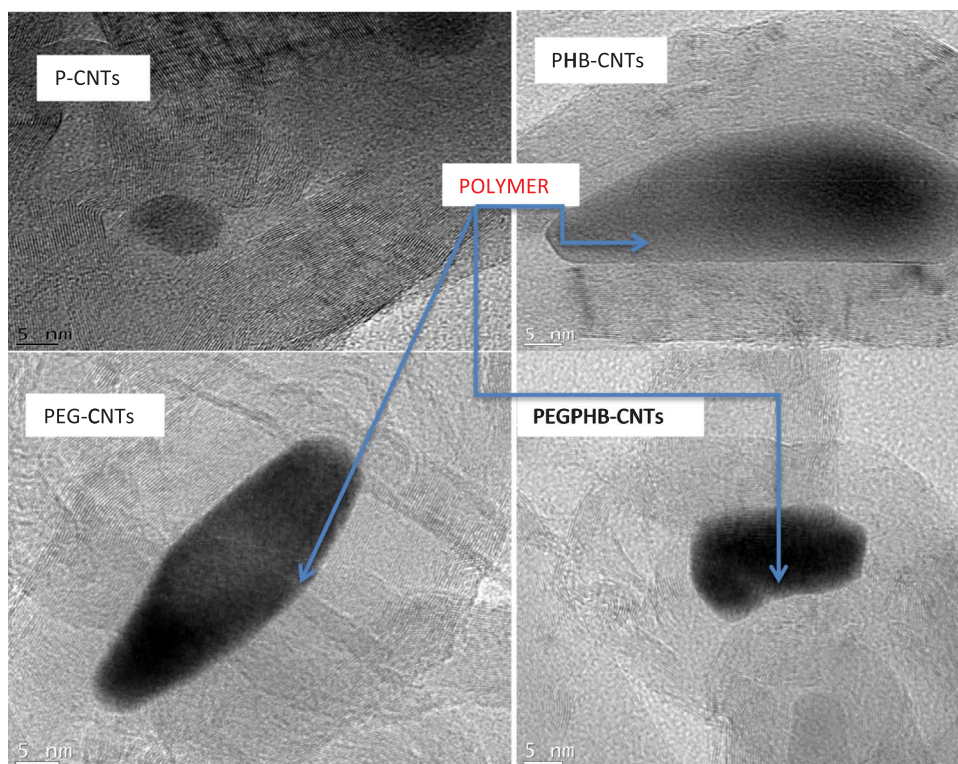


Fig. 3. High resolution transmission electron microscope images of the functionalised carbon nanotubes.

**Table 2**  
Energy dispersive x-ray spectroscopy graphs of the purified and functionalized carbon nanotubes.

Atomic (%)	P-CNTs	PHB-CNTs	PEG-CNTs	PEG-PHB-CNTs
C	93.00	93.4	93.93	94.53
O	4.13	4.30	3.74	3.07
Ca	0.06	–	–	–
Fe	0.80	0.74	0.68	0.63
Co	0.57	0.57	0.61	0.40
S	1.44	0.99	1.04	1.37
	100	100	100	100

**Table 3**  
Brunauer-Emmett-Teller (BET) Analysis Results of the Functionalized Carbon nanotubes.

Nanomaterial	Specific surface area (m <sup>2</sup> /g)	Total surface area (m <sup>2</sup> )	Total pore volume (cm <sup>3</sup> /g)	Pore radius (nm)
P-CNTs	227.64	100.16	0.08	3.16
PEG-CNTs	106.29	43.58	0.05	2.69
PHB-CNTs	253.19	111.40	0.09	3.29
PEGPHB-CNTs	148.76	44.63	0.06	2.85

properties of PHB were also reflected in the PEGPHB-CNTs, on the other hand PEG contains oxygen and amino groups which make it water soluble [32]; hence responsible for PEG-CNTs to have lower surface area and porosity. From Table 3, the pore size of the four nano-adsorbents is in the range of 2.69–3.16 nm, which is greater than 2 nm however less than 50 nm. According to IUPAC [33] samples with pore size in the range of 2–50 nm are classified as mesoporous material, which make the developed nano-sorbents mesoporous in nature. The mineralogical phases and extent of crystallinity of the prepared adsorbents were investigated using XRD and the XRD patterns of the four samples is presented in Fig. 4

According to Fig. 4, the sharp and intense diffraction peaks observed at 25.9° (002) and 44.67° (100) represent a typical graphitic multi-walled CNT structure. The other diffraction peaks observed at 53.11° (004), 64.87° (310) and 82.33° (110) indicate the presence of carbon species from the polymers due to functionalization. The intensity of these four peaks are in order of PEGPHB-CNTs > PHB-CNTs > PEG-CNTs > Pure-CNTs. The observed phenomenon in XRD patterns closely agree with the HRSEM results shown in Fig. 1, where it was found that the polymer matrix impregnate/encapsulate on the tube-like nature of the CNTs without hampering/destroying the morphologies. Furthermore, the surface oxidation state of each element present in the prepared purified and functionalized MWCNTs were determined using XPS and the results are shown in Fig. 5

XPS measurements were performed on P-CNTs and PEGPHB-CNTs and the results are presented in Fig. 6(a–b). In Fig. 4(a), the sputtered sample of P-CNTs shows the presence of C, O, Ca, and very low concentration of N. The Argon (Ar) detected in the sample is as a result of the Ar ion beam used for sputtering. The carbon (C) was identified in the binding energy region of 285.5 eV, oxygen (O) at 535.5 eV while Ca was detected at 368 eV and N at 456.5 eV respectively. The purification of CNTs using acids resulted in oxidation of outer-wall of CNTs leading to formation of new functional groups such as oxidized oxygen of O (1s). The Ca identified in the sample originated from the catalyst support (CaCO<sub>3</sub>) used in the production of CNTs. The N and S observed originated from the HNO<sub>3</sub> and H<sub>2</sub>SO<sub>4</sub> used during purification of the CNTs. The absence of the metallic species Fe and Co suggests their presence, on the surface, at concentration below the detection limits of the instrument or that these species are covered by thick over layers.

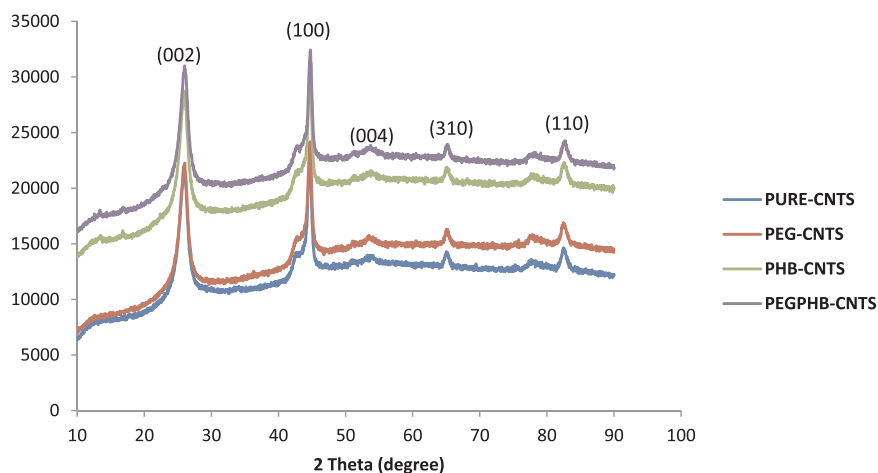


**Fig. 4.** X-ray diffraction patterns of the purified and polymer functionalised carbon nanotubes.

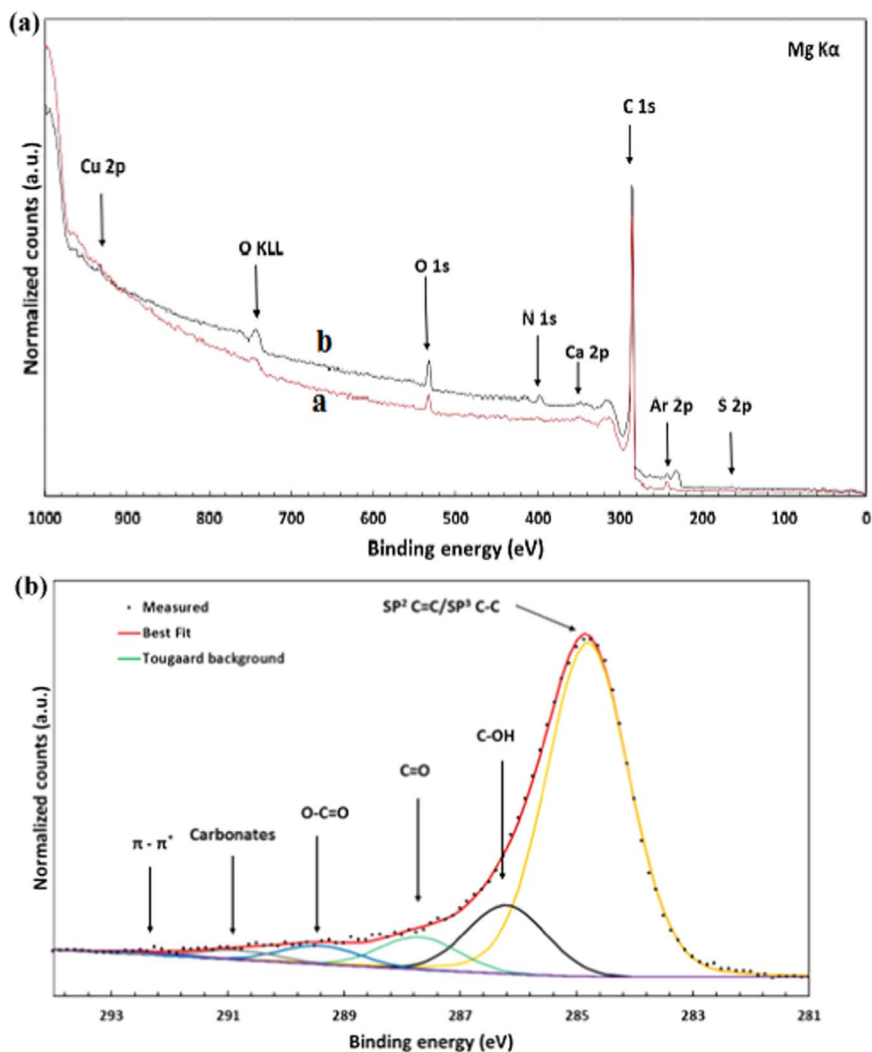


Fig. 5. (a). XPS survey scans of (a) P-CNTs and (b) PEGPHB-CNTs. (b). A typical fit for the high resolution XPS C 1s energy envelope of the P-CNTs.

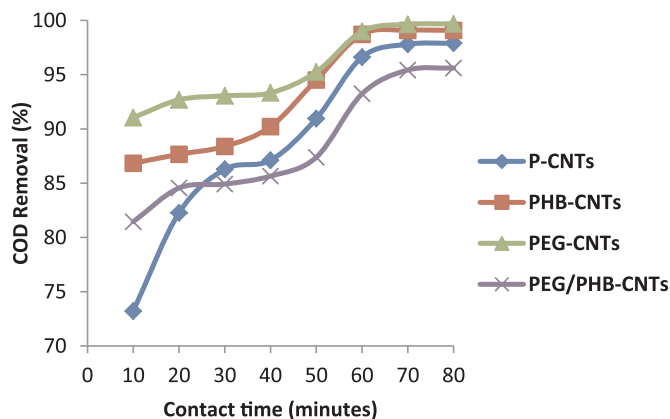


Fig. 6. Effects of contact time on COD adsorption onto pure and functionalised CNTs Experimental conditions: (adsorbent dosage (0.01 mg), agitation speed (190 rpm), and temperature (27 °C), volume of electroplating wastewater (50 cm<sup>3</sup>), stirring time (80 min).

In Fig. 5(a), the sputtered PEGPHB-CNTs revealed the presence of C, O, Ca, and weak peak of S at 182 eV. The Cu peak did not originate from the sample but rather from the adhesive tape used during analysis. Although, the EDS spectra in Table 2 shows the presence of small atomic percentage of Fe and Co. these two elements were not recorded by XPS possibly due to their low

concentrations or that these elements were not present on the surface of the MWCNTs but rather encapsulated within the wall of the CNTs as evident in the HRSEM analysis (see Fig. 1).

A typical high resolution XPS spectrum for the C 1s peak is shown in Fig. 5(b). Similar fit results were recorded for both the P-CNTs and the PEGPHB-CNTs. The results are summarized in Table 4. The C (1s) peak at 284.8 eV (P-CNTs) and 284.65 eV (PEGPHB-CNTs) is assigned to the graphitic structure of MWCNTs. The peaks at 287.7, 289.4 and 290.8 eV (P-CNTs) and 287.55, 289.25, and 290.65 eV (PEGPHB-CNTs) correspond to the attachment of carbonyl and carboxyl group to the CNTs surface during purification and functionalization.

Furthermore, the peak at 292.3 eV (P-CNTs) and 292.15 eV (PEGPHB-CNTs) are the transition loss peaks, which is assigned to  $\pi$ - $\pi^*$  and denote the chemical force of attraction on the surface of the CNTs. Contrary to P-CNTs, the total deposit of polymer on the PEGPHB-CNTs is 37,542 (69.5%), which shows that high ratio of the polymer was in-planted on the fringes of the CNTs (see Fig. 3). This invariably aids in the incorporation of more functional group that will enhance the sorption ability of the nano-adsorbent. Moreover, full width at half maximum (FWHM) of the P-CNTs compared to the PEGPHB-CNTs remain constant except for the decrease in C–C and C=C and increase in  $\pi$ - $\pi^*$ .

### 3.2.1. Effects of contact time on COD reduction

Fig. 6 illustrates the effect of contact time on COD uptake on the four nano-adsorbents. The adsorbents exhibited similar adsorption behavioral patterns; however, their rate of adsorption differs. The percentage removal of COD increases with increasing contact time and a biphasic kinetics is observed in each case. The removal rate is at first instantaneous followed by a rapid removal within the first 60 min due to a large number of available surface sites, representing the fast phase. The second phase is a slower adsorption phase process and contributed to smaller uptake of COD and finally equilibrium was reached at 70 min when most of the adsorption sites were already saturated to maximum uptake capacity. A contact time of 70 min is regarded as the optimum time for adsorption irrespective of the nano-adsorbents. After 70 min contact time, the amount of COD removed remained constant for all the adsorbents, which might be attributed to saturation of the adsorption sites as contact time increased. A similar trend was reported by Wu et al. [34] who suggested that the biphasic mechanism basically involves external and internal diffusion processes. The maximum percentage removal of COD varies and depends on the adsorbent. For instance, PEG-CNTs exhibited the highest percentage removal and was able to remove 99.68% COD within 70 min while PEGPHB-CNTs reached 95.42%. The order of maximum COD removal by the nano-adsorbents at optimum time of 70 min are as follows: PEG-CNTs (99.68%) > PHB-CNTs (97.89%) > P-CNTs (96.34%) > PEG/PHB-CNTs (95.42%).

### 3.2.2. Effects of adsorbent dosage

Fig. 7 represents the effect of adsorbent dosage on the percentage COD removal from 50 cm<sup>3</sup> electroplating wastewater after 70 min. Except for the PEGPHB-CNTs the percentage removal of COD increases very slightly as the adsorbent dosage increases and reached equilibrium at dosages of 20 mg. It is clear that the dosage needed for equilibrium is much higher for PEGPHB. All other adsorbents reached equilibrium already at a dosage of 10 mg while PEGPHB needs almost double the dosage before equilibrium. From Fig. 7 the site/area argument is maybe valid for the PEGPHB until 20 mg. The increase in the adsorption of the COD by the PEGPHB-CNTs may be ascribed to availability of more binding sites and high surface area (see Table 4). After the addition of 40 mg, there was no significant change in the COD removal irrespective of adsorbents, which may be linked to aggregation of binding sites and perhaps decrease in total adsorbent surface area of particles available to COD [35].

### 3.2.3. Effects of temperature

Fig. 8 shows the COD removal efficiency from the electroplating wastewater as a function of solution temperature. It was found that the COD removal rate decreases with increasing solution temperature, suggesting the exothermic nature of the adsorption process. This implies that as the temperature increases, the sticking coefficient of the adsorbate molecules decreases across the external boundary layer and internal pores of the adsorbent molecule. The decrease can also be linked to the swelling behavior and increased viscosity of the nano-adsorbents in the solution. In addition, increase in temperature perhaps caused decrease in binding force between the adsorbent and adsorbate and subsequently responsible for the reduction in adsorbents adsorption capacity at high temperature [36]. The findings of this study closely agree with Malana et al. [37] who used polymeric gel as adsorbent. The order of

**Table 4**  
C(1s) peak fitting results obtained for P-CNTs and PEGPHB-CNTs.

Energy (P-CNTs) (eV)	Energy (PEGPHB-CNTs) (eV)	FWHM (P-CNTs)	FWHM (PEGPHB-CNTs)	Area (P-CNTs)	Area (PEGPHB-CNTs)	Atomic % concentration (P-CNTs)	Atomic % concentration (PEGPHB-CNTs)	Chemical bonds
284.8	284.65	1.67	1.53	12,194	36,931	74.02	68.37	C–C, C=C
286.2	286.05	1.60	1.60	2232	9391	13.55	17.39	C–OH
287.7	287.55	1.60	1.60	1059	3612	6.43	6.69	C=O
289.4	289.25	1.60	1.60	604	2244	3.67	4.15	O–C=O
290.8	290.65	1.60	1.60	308	1314	1.87	2.43	Carbonates
292.3	292.15	1.50	1.60	76	523	0.46	0.97	$\pi$ - $\pi^*$
<b>Total</b>				16,473	54,015	100	100	

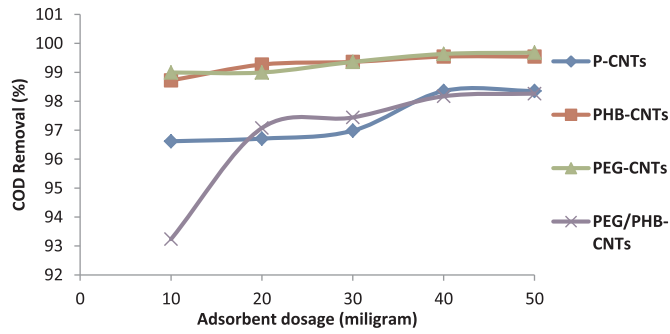


Fig. 7. Effects of pure and functionalized CNTs dosage on COD removal. (Experimental conditions: agitation speed (190 rpm), and temperature (27 °C), volume of electroplating wastewater (50 cm<sup>3</sup>), stirring time (70 min).

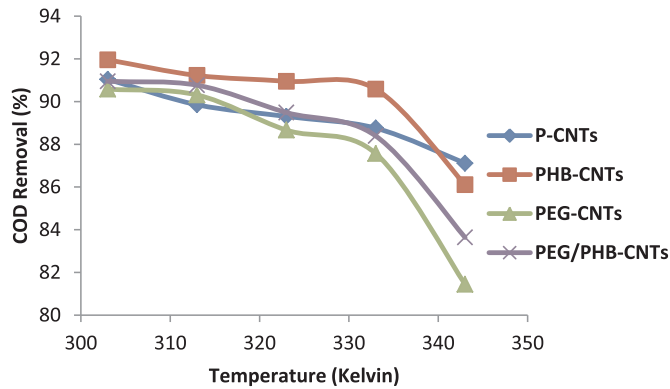


Fig. 8. Effects of temperature on COD adsorption onto pure and functionalised CNTs (adsorbent dosage 0.02 mg, agitation speed (190 rpm), volume of electroplating wastewater (50 cm<sup>3</sup>) and stirring time (70 min).

COD removal rate by the adsorbent are: PHB-CNTs > P-CNTs > PEGPHB-CNTs > PEG-CNTs. This result is in agreement with the work of Garg et al. [30].

### 3.3. Adsorption isotherm model

The adsorption isotherm is usually applied to describe the equilibrium relationship between the distribution behavior of the adsorbed molecules in both the liquid and solid phase during the adsorption process. In the present study, the Langmuir and Freundlich isotherms were applied to describe the equilibrium data obtained during the batch adsorption of COD from electroplating wastewater based on the variation of the adsorbent dosage [7]. These two models are most frequently utilized to describe the experimental data and the adsorptive capacity of the adsorbents. The Langmuir isotherm assumption remains the best known of all and describe the monolayer adsorption on a surface with homogeneous binding sites with no interaction between adsorbed species. It is expressed as follow in Eq. (3)

$$q_e = \frac{q_m K C_e}{1 + K C_e} \tag{3}$$

And on inversion, Eq. (3) becomes

$$\frac{C_e}{q_e} = \frac{1}{q_m K} + \frac{C_e}{q_m} \tag{4}$$

Where  $q_e$  is the equilibrium concentration of adsorbate in solution after adsorption (mg/g),  $C_e$  is the concentration of liquid in equilibrium with that of the solid phase (mg/L),  $q_m$  stands for the maximum adsorption capacity that corresponds to complete monolayer coverage.  $K$  represents the empirical constant from the Langmuir model that is related to the adsorption energy (L/mg). A plot of  $\frac{C_e}{q_e}$  against  $C_e$  will give a straight line, if the adsorption data fits the Langmuir isotherm.  $q_m$  and  $K$  values can be estimated from the slope and intercept respectively. Similarly, the Freundlich isotherm assumes the existence of a purely empirical relationship on a heterogeneous surface where maximum exponential distribution of adsorption sites and energies occurred. It is mostly expressed as

$$q_e = K_f C_e^{\frac{1}{n}} \tag{5}$$

The introduction of log transformed Eq. (5) to Eq. (6)

$$\ln q_e = \ln K_f + \frac{1}{n} \ln C_e \quad (6)$$

A plot of  $\ln q_e$  versus  $\ln C_e$  will give a straight line, indicating a perfect fits to the Freundlich isotherm for adsorption process.  $q_e$  is the quantity of solute adsorbed at equilibrium (mg/g),  $C_e$  is the adsorbate concentration at equilibrium. The values of  $K_f$  and  $1/n$  which are the (Freundlich empirical constants) can be evaluated from the intercept and slope respectively.  $K_f$  is a constant (Freundlich capacity factor) while  $1/n_f$  is the Freundlich intensity parameter. As mentioned earlier, the experimental data obtained via the variation of the adsorbent dosage was used to describe the equilibrium relationship between the adsorbents namely; (P-CNTs, PEG-CNTs, PHB-CNTs and PEGPHB-CNTs) and the adsorbate (COD). Table 5 gives the isothermal adsorption parameters obtained from the linearized form of the two isotherms with respect to each adsorbent.

According to Table 5, it can be noticed that the correlation coefficient ( $R^2$ ) values for both Langmuir and Freundlich isotherm are adsorbents specific. For instance, the  $R^2$  value of Langmuir isotherm for PEG-CNTs is greater than others such as P-CNTs, PHB-CNTs and PEG/PHB-CNTs. Similar trend was observed for Freundlich isotherm using the same adsorbents for COD reduction. Comparing the two isotherms with respect to correlation coefficient ( $R^2$ ) values, it can be stated that the sorption equilibrium data of COD removal from electroplating wastewater onto the nanosorbents, to a certain extent can be described by Freundlich model for all the nano-adsorbents than Langmuir model. This is because of the correlation coefficient ( $R^2$ ) values of ( $> 0.91$ ) depicts that Freundlich isotherm gave better representation of the sorption data than the Langmuir model. This result therefore suggests the formation of multilayer coverage of COD molecules at the outer surface of the nano-adsorbents which is in agreement with the work of Garg et al. [38]. In addition, the value of  $1/n_f$  obtained with all the adsorbent, which is less than 1, further support the fact that, adsorption took place homogeneously on the surface of the adsorbents. The value of  $n_f$ , for all the nano-adsorbents, falls within the range 1–10 which also indicates favorable adsorption according to Ayanda et al. [39]. Also in Table 5, it can be observed that the  $k_f$  value which corresponds to adsorption capacity of each nano-adsorbent is in order of PEG-CNTs > PHB-CNTs > PEGPHB-CNTs > P-CNTs. The adsorption trend obtained is not surface area specific (see Table 3) but rather probably due to the water holding capacity and functionality of each polymer relative to unfunctionalised P-CNTs.

### 3.4. Adsorption kinetics

Several kinetic models have been used to establish the adsorption mechanism and have better understanding of rate controlling step of the adsorption of adsorbate onto the adsorbents. Kinetics of COD sorption defines the efficiency of an adsorbent as a function of number of particles adsorbed per unit time. This can be controlled using different independent processes such as bulk diffusion, external mass transfer and intraparticle diffusion. These kinetic models include; such as Lagergren pseudo first order, pseudo second order model, the Elovich model, intraparticle diffusion model mostly interested in the influence of parameters on the overall reaction rate [40,41]. However, for this study, the first three models were chosen to interpret the sorption rate of COD onto the nano-adsorbents. The pseudo first order equation proposed by Lagergren involved the adsorption of adsorbate by the adsorbent in a system. In this model, the rate of occupation of the binding sites by the adsorbate is linearly proportional to the number of the unoccupied sites on the surface of the adsorbent. The pseudo-first order equation is normally expressed as follows:

$$\frac{d}{dt} q_t = k_1 (q_e - q_t) \quad (7)$$

Where,  $q_e$  and  $q_t$  are the amounts of metal ion adsorbed (mg/g) at equilibrium time and at any instant of time,  $t$  respectively, and  $k_1$  ( $\text{min}^{-1}$ ) is the rate constant of the pseudo first order adsorption operation deduced from the slope of the graph. The integration of Eq.

**Table 5**  
Isotherms constants for the adsorption of COD on pure and functionalised carbon nanotubes.

Equilibrium models	P-CNTs	PHB-CNTs	PEG-CNTs	PEGPHB-CNTs
<b>Langmuir</b>				
$q_m$ (mg/g)	0.0573	0.1943	0.3292	0.5615
$K$ (L/mg)	0.4625	0.9292	0.97105	0.6232
$R^2$	0.8285	0.9125	0.9406	0.8096
<b>Freundlich</b>				
$k_f$	0.0200	0.1145	0.2908	0.0479
$1/n_f$	0.7118	0.6813	0.9523	0.9093
$R^2$	0.9299	0.9305	0.9718	0.9164

(7) taken into cognizance the following boundary conditions,  $t=0$  to  $t=t$  and  $q_t=0$  to  $q_t=Q_t$ , then Eq. (7) becomes Eq. (8)

$$\ln(q_e - q_t) = \ln q_e - k_1 t \tag{8}$$

A plot of  $\ln(q_e - q_t)$  as a function of time should give a straight line for the data that fit this model. The value of  $k_1$  and  $q_e$  can be obtained from the slope and intercept respectively.

While the pseudo second order adsorption kinetic rate equation is generally expressed as

$$\frac{dq_t}{dt} = k_2(q_e - q_t)^2 \tag{9}$$

where,  $k_2$  ( $g\ mg^{-1}\ min^{-1}$ ) is the second order rate constant. On integration of the Eq. (9) using the following boundary conditions:  $t = 0$  to  $t = t$  and  $q_t = 0$  to  $q_t = q_t$ , then Eq. (9) becomes Eq. (10)

$$\frac{1}{q_e - q_t} = \frac{1}{q_e} + k_2 t \tag{10}$$

The rearrangement of Eq. (10) in a linear form is expressed as follow:

$$\frac{t}{q_t} = \frac{1}{k_2 q_e^2} + \left(\frac{1}{q_e}\right)t \tag{11}$$

where,  $h_0 = k_2 q_e^2$  can be regarded as the initial sorption rate as  $t \rightarrow 0$ . Under such circumstances, Eq. (11) reduces to

$$\frac{t}{q_t} = \frac{1}{h_0} + \left(\frac{1}{q_e}\right)t \tag{12}$$

A plot of  $t/q_t$  versus  $t$  gives a linear relationship, which allows the computation of  $q_e$ ,  $k_2$  and  $h$ . The slope gives  $\frac{1}{q_e}$  while  $k_2$  can be obtained from the intercept. The Elovich kinetic equation is a rate equation based on the adsorption capacity which is generally expressed as:

$$\frac{dq_t}{dt} = \alpha \exp(-\beta q_t) \tag{13}$$

Where  $\alpha$  ( $mg\ g^{-1}\ min^{-1}$ ) is the initial adsorption rate and  $\beta$  ( $g/mg$ ) is the desorption constant related to the extent of the surface coverage and activation energy for chemisorption. Eq. (13) is simplified by assuming  $\alpha\beta t \gg 1$  and by applying the boundary conditions  $q_t = 0$  at  $t = 0$  and  $q_t = q_t$  at  $t = t$ , as shown in Eq. (13): Thus Eq. (13) becomes

$$q_t = \frac{1}{\beta} \ln(\alpha\beta) + \frac{1}{\beta} \ln t \tag{14}$$

A plot of  $q_t$  versus  $\ln t$  should give a straight line if the sorption data fits the Elovich model.

The slope and intercept of the plot of  $q_t$  versus  $\ln t$  give the kinetic constants,  $\frac{1}{\beta}$  while the value of  $\beta$  can be obtained from the intercept. The equilibrium data obtained for the removal of COD from electroplating wastewater expressed using pseudo-first, pseudo-second order and Elovich equation are shown in Figs. 9–11 respectively. The observable parameters from various kinetic model are listed in Table 6.

The results in Table 6 shows that from the three kinetic models tested on the sorption of COD onto the nano-adsorbents, only pseudo-second order model best described the adsorption kinetics compared to other models based on the correlation coefficient ( $R^2$ ) value. This shows that the sequestration of COD as a function of kinetic models is of the order pseudo-second kinetic model > Elovich model > pseudo-first kinetic model. This is because the correlation coefficient ( $R^2$ ) value obtained for pseudo-second order model is greater than others irrespective of the nano-adsorbents and means that the adsorption mechanism followed second order kinetics. The orders of fitness to pseudo second order kinetics by the adsorbents are as follow: PEG-CNTs > PHB-CNTs > P-CNTs > PEGPHB-CNTs.

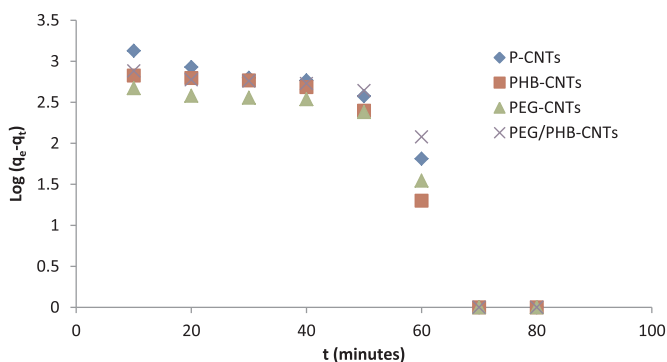


Fig. 9. Pseudo first order rate equation plot for COD adsorption on pure and functionalised carbon nanotubes.

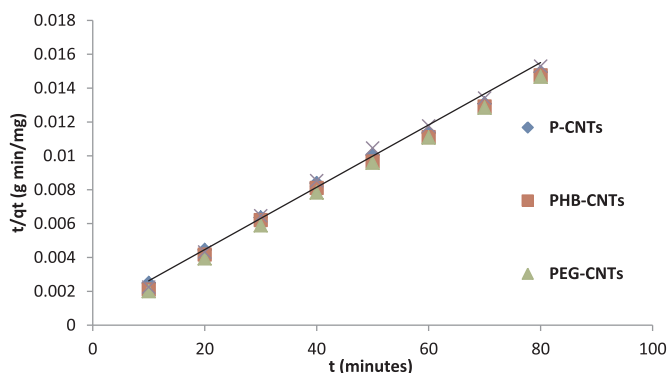


Fig. 10. Pseudo second order rate equation plot for COD adsorption on pure and functionalized carbon nanotubes.

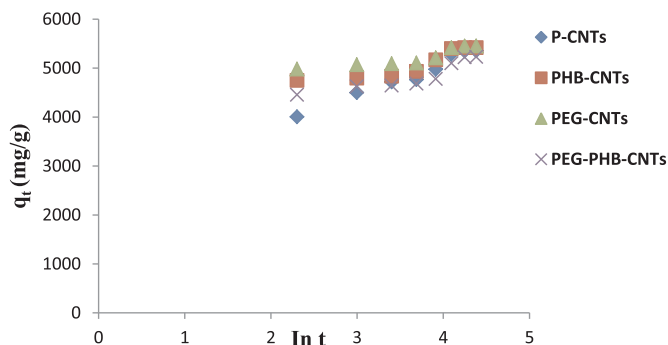


Fig. 11. Elovich rate equation plot for COD adsorption on pure and functionalized carbon nanotubes.

Table 6

Kinetic parameters for the adsorption of COD on pure and functionalized carbon nanotubes.

Kinetic parameters	P-CNTs	PHB-CNTs	PEG-CNTs	PEGPHB-CNTs
<b>Pseudo first order</b>				
$K_{ad}$ ( $\text{min}^{-1}$ )	0.1089	0.1055	0.0953	0.0993
$q_e$ (mg/g)	13436	8061	4446	8353
$R^2$	0.7998	0.8122	0.7696	0.7146
<b>Pseudo second order</b>				
$k_2$ (g/mg/min)	$4 \times 10^{-5}$	$5.716 \times 10^{-5}$	$1 \times 10^{-4}$	$5 \times 10^{-5}$
$q_e$ (mg/g)	4950	4987	5000	4968
$h$ (mg/g/min)	1000	1429	2500	1250
$R^2$	0.9971	0.9972	0.9986	0.9952
<b>Elovich</b>				
$\beta$ (g min/mg)	0.0015	0.0027	0.0041	0.0026
$\alpha$ ( $\text{g min}^2/\text{mg}$ )	$2.7 \times 10^4$	$7.3 \times 10^6$	$1.4 \times 10^{10}$	$3.5 \times 10^6$
$R^2$	0.9701	0.8053	0.8010	0.8000

Again, the observed trend may be attributed to the differences in water holding capacity of the polymers and not to the nature of their surface area. This implies that the amount of COD removed depends on the nature of nano-adsorbents. The value of the initial adsorption rate ( $h$ ), decreased as follows: 2500 mg/g/min (PEG-CNTs) > 1429 mg/g/min (PHB-CNTs) > 1250 mg/g/min (PEGPHB-CNTs) > 1000 mg/g/min P-CNTs which indicate that PEG-CNTs adsorb COD more rapidly than other nano-adsorbents. It

Table 7

Comparison of the as-prepared acid purified and polymer functionalized CNTs.

Nano-adsorbents	Maximum COD removal efficiency at 70 min (%)	Freundlich intensity parameter ( $1/n_d$ )	Pseudo-second order rate constant ( $k_2$ ) ( $:\text{gmg}^{-1}\text{min}^{-1}$ )
P-CNTs	96.34	0.71	$4.0 \times 10^{-5}$
PEG-CNTs	99.68	0.95	$1.0 \times 10^{-4}$
PHB-CNTs	97.89	0.68	$5.7 \times 10^{-5}$
PEG/PHB-CNTs	95.42	0.90	$5 \times 10^{-5}$

worthy to note that the initial adsorption rate obtained using PEG-CNTs is twice that found for PEGPHB-CNTs. This shows that the incorporation of PHB into the lattice structure of PEG-CNTs suppress the adsorption ability of PEGPHB-CNTs and responsible for its low initial adsorption rate. The high adsorption rate of PEG-CNTs compared to others may be due to the presence of nitrogen which possibly donate lone pairs of electron and bind more constituents in wastewater than PHB-CNTs without nitrogen. In principle, the pseudo second order kinetic model depends on the assumption that chemisorption is the rate-limiting step for the adsorption of COD on the nano-adsorbents, which implies that the COD ions stick to the nano-adsorbent surface and ion exchange mechanism occurred and adsorption sites became maximize [42]. Furthermore, the efficiency of the adsorbents reported in this study are compared in order to establish the most superior under the applied experimental conditions. Table 8 shows the maximum COD removal at equilibrium time of 70 min, the Freundlich intensity parameter and the pseudo-second order rate constant.

According to Table 7, it can be seen that PEG-CNTs significantly reduced COD level in the electroplating wastewater than others with (COD removal > 99%). Furthermore, the Freundlich intensity and pseudo-second order rate constant value are also suggesting the suitability of PEG-CNTs for successful removal of COD than other prepared adsorbents.

### 3.5. Adsorption thermodynamics

The change in temperature directly affect the sequestration of adsorbate by the adsorbent since adsorption phenomenon is a considered a reversible process. The influence of temperature aids in the evaluation of the change in free energy ( $\Delta G^\circ$ ), enthalpy of adsorption ( $\Delta H^\circ$ ) and entropy ( $\Delta S^\circ$ ). The free energy change (Van't Hoff equation) was estimated using the equation proposed by de la Rosa et al. [33] and Sun et al. [34] respectively.

$$\Delta G^\circ = -RT \ln K_c \quad (15)$$

$T$  (K) denotes the absolute temperature;  $R$  is the universal gas constant (8.314 J/mol/K). The equilibrium constant ( $K_c$ ) was evaluated using the relationship shown in Eq. (16)

$$K_c = C_{ad}/C_e \quad (16)$$

Where  $C_e$  and  $C_{ad}$  are the equilibrium concentrations of COD (mg/L) in solution and on adsorbent respectively. The Gibbs free energy ( $\Delta G$ ) also relates to the change in heat of adsorption ( $\Delta H^0$ ) and entropy ( $\Delta S^0$ ) at constant temperature by:

$$\Delta G^0 = \Delta H^0 - T\Delta S^0 \quad (17)$$

**Table 8**  
Thermodynamic parameters for adsorption of COD on pure and functionalized carbon nanotubes.

Temperature (°C)	$\Delta G^0$ (kJ/mol)	$\Delta S^0$ (kJ/ mol/ K)	$\Delta H^0$ (kJ/mol)	$K_c$
<b>P-CNTs</b>		35.77	7165.45	
30	-18002.25			$1.2692 \times 10^3$
40	-18359.90			$1.1590 \times 10^3$
50	-18717.55			$1.0643 \times 10^3$
60	-19075.20			$0.9823 \times 10^3$
70	-19432.85			$0.9109 \times 10^3$
<b>PHB-CNTs</b>		50.26	9896.75	
30	-25127.08			$2.1471 \times 10^4$
40	-25629.73			$1.8938 \times 10^4$
50	-26132.38			$1.6835 \times 10^4$
60	-26635.03			$1.5071 \times 10^4$
70	-27137.68			$1.3579 \times 10^4$
<b>PEG-CNTs</b>		72.53	13690.21	
30	-35668.35			$1.4097 \times 10^6$
40	-36393.70			$1.1851 \times 10^6$
50	-37119.05			$1.0069 \times 10^6$
60	-37844.40			$0.8640 \times 10^6$
70	-38569.75			$0.7480 \times 10^6$
<b>PEGPHB-CNTs</b>		45.06	-12043.74	
30	-25696.92			$2.6922 \times 10^4$
40	-26147.52			$2.3107 \times 10^4$
50	-26598.12			$2.0023 \times 10^4$
60	-27048.72			$1.7500 \times 10^4$
70	-27499.32			$1.5416 \times 10^4$

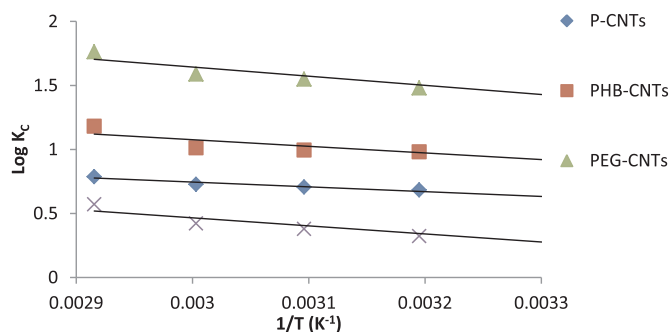


Fig. 12. A Van't Hoff plot for the adsorption of COD on pure and functionalized carbon nanotubes.

On substituting Eq. (17) into Eq. (15), gives

$$\text{Log}K_C = \frac{\Delta G^0}{RT} = \frac{\Delta S^0}{2.303R} - \frac{\Delta H^0}{2.303R} \left\{ \frac{1}{T} \right\} \quad (18)$$

The values  $\Delta H^0$  and  $\Delta S^0$  were estimated from the slopes and intercepts of a linear Van't Hoff's plot of  $\text{Log} K_C$  versus  $(1/T)$  shown in Fig. 12.

The thermodynamic parameters obtained are shown in Table 7. The negative value of  $\Delta G^0$  implies a decrease in Gibbs energy and the spontaneity of the adsorption processes. In addition, the positive value of enthalpy ( $\Delta H^0$ ) over the entire range of temperature indicates the endothermic nature of the adsorption process. The gradient of the graph is negative which means the enthalpy is positive according to Eq. (15). The enthalpy is an indication of the activation energy for diffusion. The absolute value determines the diffusion coefficient. The higher this value the lower the diffusion coefficient of adsorbate molecules across the external boundary layer and internal pores of the adsorbents. The positive value of entropy,  $\Delta S^0$  suggests an increase in degree of randomness of the adsorbed COD during the adsorption process. This further indicates an increase in randomness at the sorbent/sorbate interface during the sorption process. There is an increase in  $K_c$  with increase in temperature, which may be attributed to the increase in the adsorptive forces between the active sites of the nano-adsorbents and adsorbate species and also between the adjacent molecules of the adsorbed phases.

#### 4. Conclusions

In this study, the adsorptive potentials of pure and functionalised carbon nanotubes prepared via wet impregnation and CVD method for the removal of COD from electroplating wastewater were investigated. The results of various characterization of the nano-adsorbents revealed that the formation of a well-dispersed, poly-crystalline and multifunctional carbon nanotubes of high surface area. It was established the contact time and adsorbent dosage are directly proportional and enhanced the COD removal efficiency compared to the applied temperature which affect the removal of the indicator parameter. The COD removal efficiency was in order of PEG-CNTs > P-CNTs > PHB-CNTs > PEGPHB-CNTs and the performance of the adsorbent is not surface area specific but rather dependent on the individual water holding capacity of each material. The equilibrium and kinetic data are best described using Freundlich isotherm and pseudo second order model. The thermodynamic analysis showed that the adsorption process was exothermic and spontaneous in nature. The result of this study showed that carbon nanotubes functionalised with polyethylene glycol may be most effective adsorbent for the treatment of electroplating wastewater.

#### Acknowledgments

Financial support received from Tertiary Education Tax Fund (TETFUND) Nigeria with grant number TETFUND/FUTMINNA/NRF/2014/01 is greatly appreciated. The authors are grateful to Centre for Genetic Engineering and Biotechnology, Federal University of Technology, Minna for the assistance rendered during sample analysis. The authors wish to appreciate the following people that helped in analysing the samples: Dr Remy Bucher (XRD, ithemba Labs), Dr. Franscious Cummings (HRTEM, Physics department, University of the Western Cape (UWC), South Africa), Prof. WD. Roos (XPS, Physics department, University of the Free State, South Africa).

#### References

- [1] N.A. Noukeu, I. Gouado, R.J. Priso, D. Ndongo, V.D. Taffou, S.D. Dibong, G.E. Ekodeck, Characterization of effluent from food processing industries and stillage treatment trial with Eichhornia crassipes (Mart.) and Panicum maximum (Jacq.), *Water Resour. Industry* 16 (2016) 1–18.
- [2] T.A. Saleh, V.K. Gupta, Photo-catalyzed degradation of hazardous dye methyl orange by use of a composite catalyst consisting of multi-walled carbon nanotubes and titanium dioxide, *J. Colloid Interface Sci.* 371 (2012) 101–106.
- [3] A. Mittal, J. Mittal, A. Malviya, V.K. Gupta, Removal and recovery of Chrysoidine Y from aqueous solutions by waste materials, *J. Colloid Interface Sci.* 344 (2010) 497–507.
- [4] M. Chowdhury, M.G. Mostafa, T.K. Biswas, A.K. Saha, Treatment of leather industrial effluents by filtration and coagulation processes, *Water Resour. Ind.* 3

- (2013) 11–22.
- [5] V.K. Gupta, R. Jain, A. Nayak, S. Agarwal, M. Shrivastava, Removal of the hazardous dye—Tartrazine by photodegradation on titanium dioxide surface, *Mater. Sci. Eng. C* 31 (2011) 1062–1067.
  - [6] R. Saravanan, E. Thirumal, V.K. Gupta, V. Narayanan, A. Stephen, The photocatalytic activity of ZnO prepared by simple thermal decomposition method at various temperatures, *J. Mol. Liq.* 177 (2013) 394–401.
  - [7] A. Mittal, J. Mittal, A. Malviya, V.K. Gupta, Adsorptive removal of hazardous anionic dye “Congo red” from wastewater using waste materials and recovery by desorption, *J. Colloid Interface Sci.* 340 (2009) 16–26.
  - [8] A. Mittal, D. Kaur, A. Malviya, J. Mittal, V.K. Gupta, Adsorption studies on the removal of coloring agent phenol red from wastewater using waste materials as adsorbents, *J. Colloid Interface Sci.* 337 (2009) 345–354.
  - [9] A.K. Jain, V.K. Gupta, A. Bhatnagar, Suhas, A comparative study of adsorbents prepared from industrial wastes for removal of dyes, *Sep. Sci. Technol.* 38 (2) (2003) 463–481, <http://dx.doi.org/10.1081/SS-120016585>.
  - [10] V.K. Gupta, R. Jain, A. Mittal, T.A. Saleh, A. Nayak, S. Agarwal, S. Sikarwar, Photocatalytic degradation of toxic dye amaranth on TiO<sub>2</sub>/UV in aqueous suspensions, *Mater. Sci. Eng. C* 32 (2012) 12–17.
  - [11] V.K. Gupta, R. Kumar, A. Nayak, T.A. Saleh, M.A. Barakat, Adsorptive removal of dyes from aqueous solution onto carbon nanotubes: a review, *Adv. Colloid Interface Sci.* 193–194 (2013) 24–34.
  - [12] R. Saravanan, V.K. Gupta, E. Mosquera, F. Gracia, Preparation and characterization of V<sub>2</sub>O<sub>5</sub>/ZnO nanocomposite system for photocatalytic application, *J. Mol. Liq.* 198 (2014) 409–412.
  - [13] T.A. Saleh, V.K. Gupta, Processing methods, characteristics and adsorption behavior of tire derived carbons: a review, *Adv. Colloid Interface Sci.* 211 (2014) 93–101.
  - [14] A. Mittal, J. Mittal, A. Malviya, D. Kaur, V.K. Gupta, Decoloration treatment of a hazardous triarylmethane dye, Light Green SF (Yellowish) by waste material adsorbents, *J. Colloid Interface Sci.* 342 (2010) 518–527.
  - [15] V.K. Gupta, T.A. Saleh, Sorption of pollutants by porous carbon, carbon nanotubes and fullerene - An overview, *Environ. Sci. Pollut. Res* 20 (2013) 2828–2843.
  - [16] H. Khani, M.K. Rofouei, P. Arab, V.K. Gupta, Z. Vafaei, Multi-walled carbon nanotubes-ionic liquid-carbon paste electrode as a super selectivity sensor: application to potentiometric monitoring of mercury ion(II), *J. Hazard. Mater.* 183 (2010) 402–409.
  - [17] V.K. Gupta, A. Mittal, D. Jhare, J. Mittal, Batch and bulk removal of hazardous colouring agent Rose Bengal by adsorption techniques using bottom ash as adsorbent, *RSC Adv.* 2 (2012) 8381–8389.
  - [18] V.K. Gupta, A. Nayak, S. Agarwal, Bioadsorbents for remediation of heavy metals: current status and their future prospects, *Environ. Eng. Res.* 20 (1) (2015) 001–018.
  - [19] F. Su, C. Lu, Adsorption kinetics, thermodynamics and desorption of natural dissolved organic matter by multiwalled carbon nanotubes, *J. Environ. Sci. Health, Part. A* 42 (11) (2007) 1543–1552.
  - [20] T.A. Saleh, V.K. Gupta, Column with CNT/magnesium oxide composite for lead(II) removal from water, *Environ. Sci. Pollut. Res* 19 (2012) 1224–1228.
  - [21] F. Su, C. Lu, S. Hu, Adsorption of benzene, toluene, ethylbenzene and p-xylene by NaOCl-oxidized carbon nanotubes, *Colloids and Surfaces A: physicochem, Eng. Asp.* 353 (2010) 83–91.
  - [22] Z.S. Veličković, Z.J. Bajić, M.D. Ristić, V.R. Djokić, A.D. Marinković, P.S. Uskoković, M.M. Vuruna, Modification of multi-wall carbon nanotubes for the removal of cadmium, lead and arsenic from wastewater, *Dig. J. Nanomater. Biostruct.* 8 (2) (2013) 501–511.
  - [23] V.K. Gupta, S. Agarwal, T.A. Saleh, Synthesis and characterization of alumina-coated carbon nanotubes and their application for lead removal, *J. Hazard. Mater.* 185 (2011) 17–23.
  - [24] T.A. Saleh, Mercury sorption by silica/carbon nanotubes and silica/activated carbon: a comparison study, *J. Water Supply: Res. Technol.-Aqua* 64 (8) (2015) 892–903.
  - [25] T.A. Saleh, Nanocomposite of carbon nanotubes/silica nanoparticles and their use for adsorption of Pb(II): from surface properties to sorption mechanism, *Desalin. Water Treat.* 57 (23) (2016) 10730–10744.
  - [26] Y. Kwon, W. Shim, S.Y. Jeon, J.H. Youk, W.R. Yu, Improving dispersion of multi-walled carbon nanotubes and graphene using a common non-covalent modifier, *Carbon Lett.* 20 (2016) 53–61.
  - [27] Fondriest Environmental, Inc., pH of Water, Fundamentals of Environmental Measurements. 19 November <<http://www.fondriest.com/environmental-measurements/parameters/water-quality/ph/>>.
  - [28] World Health Organization (WHO), Background document for preparation of WHO Guidelines for drinking-water quality. Geneva, 2003.
  - [29] Environmental Protection Agency, Monitoring and assessing water quality, volunteer stream monitoring methods Manual, Chapter 5 Section 2 Dissolved Oxygen and Biochemical Oxygen Demand, <[www.epa.gov](http://www.epa.gov)> (10/21/07).
  - [30] Nigerian Industrial Standard (NIS), Nigerian standard for drinking water quality, 16–17, 2007.
  - [31] N. Jacquet, C.W. Lo, H.S. Wu, Y.H. Wei, S.S. Wang, Solubility of polyhydroxyalkanoates by experiment and thermodynamic correlations, *AIChE J.* 53 (10) (2007) 2704–2714, <http://dx.doi.org/10.1002/aic.11274>.
  - [32] M.A. Tofighy, T. Mohammadi, Adsorption of divalent heavy metal ion using carbon nanotube sheets, *J. Hazard. Mater.* 185 (2011) 140–147.
  - [33] T.A. Saleh, V.K. Gupta, Functionalization of tungsten oxide into MWCNT and its application for sunlight-induced degradation of rhodamine B, *J. Colloid Interface Sci.* 362 (2011) 337–344.
  - [34] Y. Wu, L. Zhang, C. Gao, X. Ma, R. Han R, Adsorption of copper ions and methylene Blue in a single and Binary System on Wheat straw, *J. Chem. Eng. Data* 54 (2010) 3229–3234.
  - [35] V.K. Gupta, I. Ali, T.A. Saleh, A. Nayaka, S. Agarwal, Chemical treatment technologies for waste-water recycling—an overview, *RSC Adv.* 2 (2012) 6380–6388.
  - [36] V.K. Gupta, A. Nayak, Cadmium removal and recovery from aqueous solutions by novel adsorbents prepared from orange peel and Fe<sub>2</sub>O<sub>3</sub> nanoparticles, *Chem. Eng. J.* 180 (2012) 81–90.
  - [37] M.A. Malana, S. Ijaz, M.N. Ashiq, Removal of various dyes from aqueous media onto polymeric gels by adsorption process: their kinetics and thermodynamics, *Desalination* 263 (2010) 249–257.
  - [38] K.K. Garg, P. Rawat, B. Prasad, Removal of Cr (VI) and COD from Electroplating Wastewater by Corncob Based Activated Carbon, *Int. J. Water Wastewater Treat.* 1 (1) (2015) 1–9.
  - [39] O.S. Ayanda, O.S. Fatoki, F.A. Adekola, B.J. Ximbaa, Removal of tributyltin from shipyard process wastewater by fly ash, activated carbon and fly ash/activated carbon composite: adsorption models and kinetics, *J. Chem. Technol. Biotechnol.* 88 (2013) 2201–2208.
  - [40] X.F. Sun, S.G. Wang, X.W. Liu, W.X. Gong, N. Bao, B.Y. Gao, H.Y. Zhang, Biosorption of Malachite Green from aqueous solutions onto aerobic granules: kinetic and equilibrium studies, *Bioresour. Technol.* 99 (2008) 3475–3483.
  - [41] G. De la Rosa, H.E. Reynel-Avila, A. Bonilla-Petriciolet, I. Cano-Rodríguez, C. Velasco-Santos, R. Martínez-Elangovan, L. Pilip, K. Chandraraj, Biosorption of chromium species by aquatic weeds: kinetics and mechanism studies, *J. Hazard. Mater.* 152 (2008) 100–102.
  - [42] P.W. Atkins, Physical Chemistry, 5th ed., Oxford University Press, Oxford, 1995.